

# Single Molecular Orientation Switching of an Endohedral Metallofullerene

Yuhsuke Yasutake,<sup>†</sup> Zujin Shi,<sup>§,||</sup> Toshiya Okazaki,<sup>§,⊥</sup> Hisanori Shinohara,<sup>§</sup> and Yutaka Majima<sup>\*,†,‡</sup>

Department of Physical Electronics, Tokyo Institute of Technology, Tokyo 152-8552, Japan, SORST, Japan Science and Technology Agency, Tokyo 152-8552, Japan, and Department of Chemistry & Institute for Advanced Research, Nagoya University, Nagoya 464-8602, Japan

Received March 14, 2005; Revised Manuscript Received April 30, 2005

## ABSTRACT

The single molecular orientation switching of the Tb@C<sub>82</sub> endohedral metallofullerene has been studied by using low-temperature ultrahigh vacuum (UHV) scanning tunneling microscopy (STM). An octanethiol self-assembled monolayer (SAM) was introduced between Tb@C<sub>82</sub> and the Au(111) substrate to control the thermal rotational states of Tb@C<sub>82</sub>. Scanning tunneling spectroscopy (STS) of Tb@C<sub>82</sub> on an octanethiol SAM at 13 K demonstrated hysteresis including negative differential conductance (NDC). This observed hysteresis and NDC is interpreted in terms of a switching of the Tb@C<sub>82</sub> molecular orientation caused by the interaction between its electric dipole moment and an external electric field.

The formation of a functional structure of a desired texture on the subnanometer scale is a primary concern when designing molecular nanodevices. Single-molecular switching devices composed of a single functional molecule<sup>1–4</sup> have been extensively studied because they are likely to be employed in nanomemory device<sup>5,6</sup> and logic circuits.<sup>7–10</sup> Although these molecular switching devices utilize molecular functions, direct observations of the switching phenomena on a single molecule may prove useful in obtaining conceptual instructions for designing the molecular nanodevices in a manner similar to building a “LEGO” block. Endohedral metallofullerenes<sup>11</sup> are one of the candidate materials for creating single molecular orientation switching devices owing to their electric dipole moment<sup>12–14</sup> due to the exchange of electrons between the encapsulated metal atom and a fullerene cage. For instance, in the case of the Tb@C<sub>82</sub> (isomer I) endohedral metallofullerene, the Tb@C<sub>82</sub> cage exhibits C<sub>2v</sub> symmetry and possesses an electric dipole moment that is derived from the trivalent Tb<sup>3+</sup>C<sub>82</sub><sup>3-</sup> electronic states. The control of the texture and the orbital interactions of surrounding Tb@C<sub>82</sub> molecules on the sub-

nanometer scale is the key to realizing the single molecular orientation switching device by using Tb@C<sub>82</sub>.

Here, we report the single molecular orientation switching properties of a single Tb@C<sub>82</sub> on an octanethiol SAM that were observed by STS by using low-temperature UHV–STM. To realize this, the tunneling current (*I*)–distance (*d*) characteristics above alkanethiol SAMs on the Au(111) substrate have been measured by the scanning vibrating probe method.<sup>15,16</sup> On the basis of the *I*–*d* characteristics, we evaluate the conductance decay constants and the transconductance of the alkanethiol SAMs. *I*–*V* characteristics of the STM probe/vacuum/single Tb@C<sub>82</sub> molecule/alkanethiol SAM/Au(111) structure repeatedly demonstrate hysteresis including NDC. These hysteresis phenomena are discussed on the basis of the interaction between the electric dipole moment of Tb@C<sub>82</sub> and the external electric field.

Tb@C<sub>82</sub> (isomer I) was produced by the dc arc-discharge method followed by purification and isolation by multistage high-performance liquid chromatography.<sup>17</sup> The Au(111) substrate was fabricated by the thermal evaporation of gold onto freshly cleaved mica. Prior to gold evaporation, mica substrates were held at 500 °C for 2 h in a vacuum. The substrate temperature was kept at 450 °C during gold evaporation, and postannealing was performed at the same temperature for 8 h to form an atomically flat Au(111) surface. Each Au(111) substrate was immersed in a 1 mM solution of hexanethiol (Wako Pure Chemical Industries, Ltd., Osaka, Japan) or octanethiol (Sigma Aldrich Japan, Tokyo, Japan) in ethanol for 48 h. Tb@C<sub>82</sub> metallofullerenes

\* Corresponding author. E-mail: majima@pe.titech.ac.jp. Tel: +81-3-5734-2673. Fax: +81-3-5734-2673.

<sup>†</sup> Tokyo Institute of Technology.

<sup>‡</sup> SORST, Japan Science and Technology Agency.

<sup>§</sup> Nagoya University.

<sup>||</sup> Current address: Department of Chemistry, Peking University, Beijing 100871, China.

<sup>⊥</sup> Current address: Research Center for Advanced Carbon Materials, National Institute of Advanced Industrial Science and Technology, Tsukuba 305-8565, Japan.

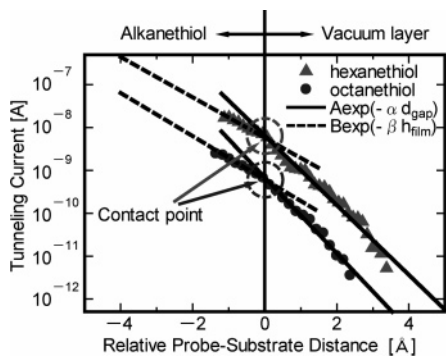


**Figure 1.** Semilogarithmic plot of  $I$ - $d$  characteristics above hexanethiol and octanethiol SAMs on Au(111). In the  $I$ - $d$  characteristic of octanethiol, the center of vibration of the STM probe is set at a set-point current of 3 pA and an STM probe vibrational amplitude of 14 Å. Similarly, the  $I$ - $d$  characteristics of hexanethiol are obtained at a set-point current of 30 pA and an STM probe vibrational amplitude of 10 Å. The STM probe bias voltage is set to  $-2$  V in both of these measurements.

were degassed at 120 °C for 12 h, and then a submonolayer of Tb@C<sub>82</sub> was sublimated at 500 °C on the octanethiol/Au(111) surface. The sample was introduced into an UHV-STM with a base pressure lower than  $1.0 \times 10^{-8}$  Pa. The STM probe was a mechanically cut PtIr probe.

On the basis of the tunneling  $I$ - $d$  characteristic measurements of alkanethiol SAMs obtained by using a scanning vibrating probe, the candidacy of alkanethiol SAMs by the two-layer tunnel model was evaluated.<sup>18</sup> Figure 1 shows the experimental results of semilogarithmic  $I$ - $d$  characteristics. The kinks in the tunneling current slopes are clearly observed in the  $I$ - $d$  characteristics of both hexanethiol and octanethiol SAMs, suggesting the contact between the top of the STM probe and the end of hexanethiol or octanethiol SAMs. Because the relative probe-substrate distance is set to zero at the kink, the STM probe penetrates the alkanethiol SAM in the negative region of relative distance, and the top of the STM probe is located in a vacuum in the positive region. The tunneling conductance at the kink can be estimated from Figure 1 to be  $3.5 \times 10^{-9}$  and  $3.4 \times 10^{-10} \Omega^{-1}$ . The conductance decay constants through hexanethiol and octanethiol SAMs ( $\beta$ ) can be obtained from the dashed line in Figure 1 to be 1.1 and 1.2 Å<sup>-1</sup>, respectively, and the conductance decay constants of the vacuum above hexanethiol and octanethiol ( $\alpha$ ) can be obtained from the solid line to be 1.9 and 2.0 Å<sup>-1</sup>, respectively. These results are in good agreement with previous reports.<sup>18,19</sup> If there exist a strong orbital interaction between a class of fullerene materials and a metal substrate, then the highest occupied molecular orbital (HOMO) and the lowest unoccupied molecular orbital (LUMO) states are modulated, and molecular motion tends to be restrained because of the strong interaction.<sup>20-23</sup> Consequently, the alkanethiol SAM is expected to be a suitable base material for measuring the rotational HOMO and LUMO properties of Tb@C<sub>82</sub> and designing the device structure on a subnanometer scale.

Figure 2A and B shows the STM images of Tb@C<sub>82</sub> molecules on the octanethiol/Au(111) surface. To clarify the electric property of a single Tb@C<sub>82</sub> molecule, it is important

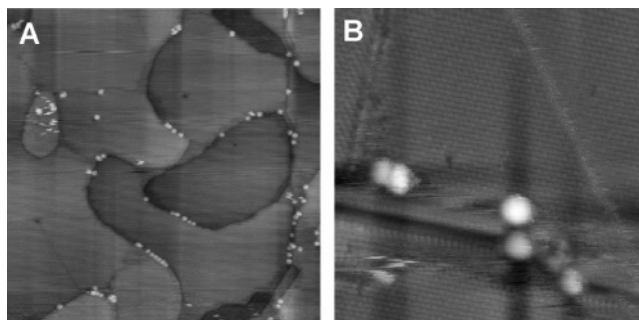


**Figure 2.** STM image of Tb@C<sub>82</sub> absorbed on an octanethiol/Au(111) surface at 299 K. (A) Scan size = 120 × 120 nm<sup>2</sup>, probe bias voltage ( $V_p$ ) =  $-1.7$  V, and set-point current ( $I_T$ ) = 1.7 pA. (B) Scan size = 20 × 20 nm<sup>2</sup>,  $V_p$  =  $-1.8$  V, and,  $I_T$  = 12 pA.

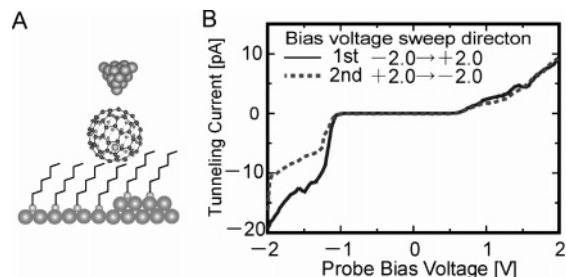


**Figure 3.** (A) Schematic image of a double-barrier tunnel junction (DBTJ) that consists of the PtIr probe/vacuum/Tb@C<sub>82</sub>/hexanethiol SAM/Au(111) substrate. (B) Typical  $I$ - $V$  characteristics of Tb@C<sub>82</sub> in the double-barrier tunnel junction, where  $V_p$  =  $-2$  V,  $I_T$  = 20 pA, and  $T$  = 68 K. The solid lines represent  $I$ - $V$  characteristic of the  $V_p$  sweep direction from negative to positive, and the dashed lines represent  $I$ - $V$  characteristic of the  $V_p$  sweep direction from positive to negative. Each  $I$ - $V$  line represents the average of six  $I$ - $V$  characteristics.

to control the aggregation of Tb@C<sub>82</sub> molecules. In Figure 2, bright points represent individual Tb@C<sub>82</sub> molecules. From these STM images, we conclude that Tb@C<sub>82</sub> can diffuse on the octanethiol SAM surface; furthermore, it can be trapped along the Au(111) monatomic step edge (Figure 2A) and at the etch pit and grain boundary (Figure 2B), which is caused by the chemical absorption of the alkanethiol SAM. These molecular diffusions are due to the weak bond caused by the van der Waals interaction between molecules and the alkanethiol SAM.

Figure 3A shows a schematic image of the sample structure that forms the double barrier tunnel junction. Figure 3B shows the typical  $I$ - $V$  characteristics of a single Tb@C<sub>82</sub> molecule absorbed onto a hexanethiol SAM by STS at 68 K. In Figure 3B, the zero-current regions that are observed in the probe bias voltage ( $V_p$ ) range from  $-0.87$  to  $0.5$  V and may be attributed to the Coulomb gap. It should be noted that the electron transport through a single molecule with two tunneling barriers is determined by a combination of the molecular energy level and Coulomb blockade.<sup>24</sup> As shown in Figure 1, the tunneling resistance of the hexanethiol SAM is approximately  $3 \times 10^8 \Omega$ . Assuming  $R_2$  to be  $3 \times 10^8 \Omega$ ,  $R_1$  becomes larger than  $R_2$  ( $R_1/R_2 \gg 1$ ) because the voltage-tunneling current ratio is larger than  $1 \times 10^{11} \Omega$  ( $V_p = -2$  V, set-point current is 20 pA). When  $R_1/R_2 \gg 1$ , the Tb@C<sub>82</sub> molecule tends to be positively charged at the

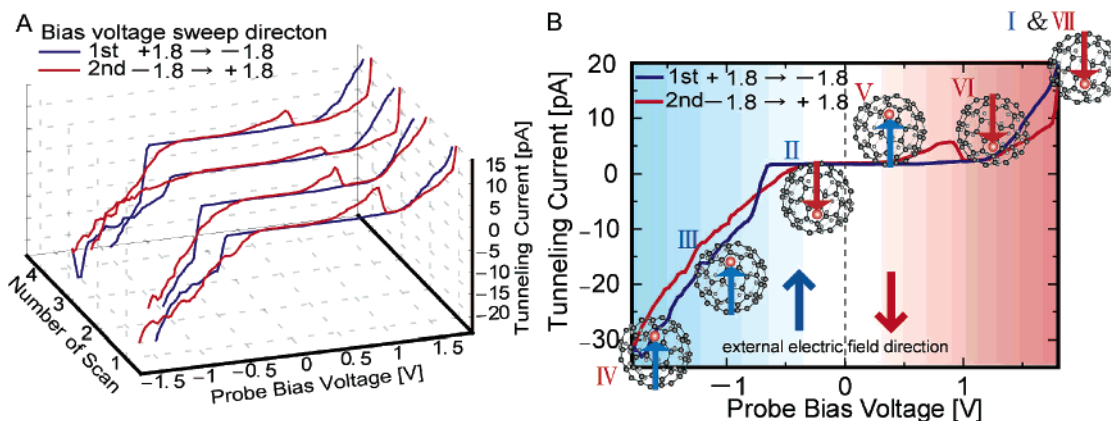


**Figure 4.** (A) Sequence of STS results of Tb@C<sub>82</sub> on octanethiol at 13 K. Initial  $V_p$  is +1.8 V and  $I_T = 20$  pA; then  $V_p$  is swept to -1.8 V and vice versa. (B) Candidate schematic image of single molecular orientation switching of Tb@C<sub>82</sub> that describes hysteresis and NDC in terms of the switching of the Tb@C<sub>82</sub> molecular orientation caused by the interaction between its electric dipole moment and an external electric field.

negative probe bias voltage and negatively charged at the positive voltage.

Figure 4A shows the sequence of STS characteristics of a single Tb@C<sub>82</sub> molecule under the  $V_p$  sweep from 1.8 to -1.8 V and vice versa at 13 K. Hysteresis and NDC have been repeatedly observed in the  $I-V$  characteristics of the single Tb@C<sub>82</sub> molecule on the octanethiol SAM/Au(111) structure at 13 K. Figure 4B shows the schematic image of single molecular orientation switching of Tb@C<sub>82</sub> that describes hysteresis and NDC in terms of a switching of the Tb@C<sub>82</sub> molecular orientation caused by the interaction between its electric dipole moment and an external electric field ( $E_{ext}$ ). As shown in Figure 3B, no hysteresis has been observed in the STS measurement at 68 K. The Tb@C<sub>82</sub> molecules are considered to be rotating because of the thermal energy of 5.9 meV at 68 K.<sup>25</sup> On the contrary, the thermal rotation of the Tb@C<sub>82</sub> molecule should terminate under the thermal energy of 1.1 meV at 13 K. As the result of the electrons transfer from the Tb atom to the carbon cage (Tb@C<sub>82</sub>), the Tb@C<sub>82</sub> molecule has a electric dipole moment. For instance, the value of the electric dipole moment of the Y<sup>3+</sup>@C<sub>82</sub><sup>3-</sup> molecule has been reported to be 2.5 D.<sup>26</sup> The electrostatic energy depends on the orientation of the electric dipole moment ( $\mu$ ) and an internal electric field ( $E_{int}$ ) in a fullerene cage, which is given by the sum of an external electric field by the probe bias voltage and an electric field due to an induced surface polarization charge on the conductive fullerene cage.<sup>27</sup> If the electrostatic energy is larger than the thermal energy, then the external electric field tends to line up the electric dipole moment of the Tb@C<sub>82</sub> molecule. On the contrary, if the electrostatic energy is smaller than the thermal energy, then the electric dipole moment of the Tb@C<sub>82</sub> molecule tend to be oriented at random. An antiparallel state will appear by sweeping the voltage if the rotation of Tb@C<sub>82</sub> is restrained at 13 K and the electrostatic energy is smaller than an activation energy where the Tb@C<sub>82</sub> molecule starts to rotate thermally. Because hysteresis has been observed in the  $I-V$  characteristics only at 13 K, the electrostatic energy due to the redirection of the Tb@C<sub>82</sub> molecule ( $2\mu E_{int}$ ) under the

internal electric field should be in the range between 1.1 and 5.9 meV, which corresponds to the internal electric field in the fullerene cage in the range between 0.011 and 0.057 V/nm by assuming  $\mu$  to be 2.5 D. This estimated internal electric field in the fullerene cage is approximately one order smaller than the external electric field assuming a probe bias voltage of 0.9 V, a relative permittivity as 1, and the distance between probe and Au(111) substrate to be 2 nm, which suggests the effect of the conductive fullerene cage.

The NDC has also been repeatedly observed in the  $V_p$  sweep direction from a negative direction to a positive direction in Figure 4A, and the mean peak probe bias voltage of the NDC is 0.9 V. At this probe bias voltage of 0.9 V, the Tb@C<sub>82</sub> molecule should start to rotate from the antiparallel state to the parallel state gradually. This NDC phenomenon should be interpreted as follows: one explanation is a change in the fractional residual charge  $Q_0$  in the double-barrier tunnel junction. Because  $Q_0$  is extremely sensitive to changes in the electrostatic environment such as the direction of the electric dipole moment, the redirection of the Tb@C<sub>82</sub> molecule tends to shift the Coulomb staircase to the voltage axis, especially at the onset voltages of current.<sup>28</sup> The other is the electronic properties of Tb@C<sub>82</sub>. Because of the off-center trivalent Tb atom along the 2-fold axis of  $C_{2v}$  symmetry, the electron density surface corresponding to the HOMO and LUMO states is also in an off-centered configuration.<sup>29</sup> When the Tb@C<sub>82</sub> molecule redirects because of the external electric field, the tunneling conductance changes because of the off-centered HOMO and LUMO states. Consequently, the  $I-V$  characteristics should exhibit hysteresis because of the asymmetric orientational redirection of the Tb@C<sub>82</sub> molecule, and the Tb@C<sub>82</sub> molecule should rotate at the peak voltage of the NDC, which occurs because of the external electric field.

In conclusion, we have demonstrated the single molecular orientation switching properties of Tb@C<sub>82</sub> by introducing octanethiol SAM as the interlayer on the Au(111) substrate. The  $I-V$  characteristics of a single Tb@C<sub>82</sub> molecule on an octanethiol SAM repeatedly exhibited hysteresis and NDC. This observed hysteresis and NDC is interpreted in terms of

a switching of the Tb@C<sub>82</sub> molecular orientation caused by the interaction between its electric dipole moment and an external electric field. Furthermore, this hysteresis and NDC has obvious relevance for single molecular switching devices that use endohedral metallofullerenes.

## References

- (1) Aviram, A.; Ratner, M. A. *Chem. Phys. Lett.* **1974**, *29*, 277.
- (2) Park, H.; Park, J.; Lim, A. K. L.; Anderson, E. H.; Alivisatos, A. P.; McEuen, P. L. *Nature* **2000**, *407*, 57.
- (3) Park, J.; Pasupathy, A. N.; Goldsmith, J. I.; Chang, C.; Yaish, Y.; Petta, J. R.; Rinkoski, M.; Sethna, J. P.; Abruna, H. D.; McEuen, P. L.; Ralph, D. C. *Nature* **2002**, *417*, 722.
- (4) Donhauser, Z. J.; Mantooth, B. A.; Kelly, K. F.; Bumm, L. A.; Monnell, J. D.; Stapleton, J. J.; Price Jr., D. W.; Rawlett, A. M.; Allara, D. L.; Tour, J. M.; Weiss, P. S. *Science* **2001**, *292*, 2303.
- (5) Reed, M. A.; Chen, J. *Appl. Phys. Lett.* **2001**, *78*, 3735.
- (6) Bandyopadhyay, A.; Pal, A. J. *Appl. Phys. Lett.* **2003**, *82*, 1215.
- (7) Aviram, A. *J. Am. Chem. Soc.* **1988**, *110*, 5687.
- (8) Joachim, C.; Gimzewski, J. K.; Aviram, A. *Nature* **2001**, *408*, 541.
- (9) Collier, C. P.; Wong, E. W.; Belohradský, M.; Raymo, F. M.; Stoddart, J. F.; Kuekes, P. J.; Williams, R. S.; Heath, J. R. *Science* **1999**, *285*, 391.
- (10) Chen, Y.; Jung, G. Y.; Ohlberg, D. A. A.; Li, X.; Stewart, D. R.; Jeppesen, J. O.; Nielsen, K. A.; Stoddart, J. F.; Williams, R. S. *Nanotechnology* **2003**, *14*, 462.
- (11) Shinohara, H. *Rep. Prog. Phys.* **2000**, *63*, 843.
- (12) Gimzewski, J. K. *Proceedings of NATO ARW on the Chemical Physics of Fullerenes 10 (and 5) Years Later*; 1996; p 117.
- (13) Nuttall, C. J.; Hayashi, Y.; Yamazaki, K.; Mitani, T.; Iwasa, Y. *Adv. Mater.* **2002**, *14*, 293.
- (14) Kornilovitch, P. E.; Bratkovsky, A. M.; Williams, R. S. *Phys. Rev. B* **2002**, *66*, 245413.
- (15) Majima, Y.; Nagano, K.; Okuda, A. *Jpn. J. Appl. Phys.* **2002**, *41*, 5381.
- (16) Nagano, K.; Okuda, A.; Majima, Y. *Appl. Phys. Lett.* **2002**, *81*, 544.
- (17) Shi, Z.; Okazaki, T.; Shimada, T.; Sugai, T.; Suenaga, K.; Shinohara, H. *J. Phys. Chem. B* **2003**, *107*, 2485.
- (18) Bumm, L. A.; Arnold, J. J.; Dunbar, T. D.; Allara, D. L.; Weiss, P. S. *J. Phys. Chem. B* **1999**, *103*, 8122.
- (19) Lee, T.; Wang, W.; Klemic, J. F.; Zhang, J. J.; Su, J.; Reed, M. A. *J. Phys. Chem. B* **2004**, *108*, 8742.
- (20) Lu, X.; Grobis, M.; Khoo, K. H.; Louie, S. G.; Crommie, M. F. *Phys. Rev. B* **2004**, *70*, 115418.
- (21) Butcher, M. J.; Nolan, J. W.; Hunt, M. R. C.; Beton, P. H. *Phys. Rev. B* **2001**, *64*, 195401.
- (22) Uemura, S.; Sakata, M.; Hirayama, C.; Kunitake, M. *Langmuir* **2004**, *20*, 9198.
- (23) Taninaka, A.; Shino, K.; Sugai, T.; Heike, S.; Terada, Y.; Hashizume, T.; Shinohara, H. *Nano Lett.* **2003**, *3*, 337.
- (24) Kubatkin, S.; Danilov, A.; Hjort, M.; Cornil, J.; Brédas, J. L.; Stuhr-Hansen, N.; Hedegård, P.; Bjørnholm, T. *Nature* **2003**, *425*, 698.
- (25) Taninaka, A.; Kato, H.; Shino, K.; Sugai, T.; Terada, T.; Heike, S.; Hashizume, T.; Shinohara, H. *e-J. Surf. Sci. Nanotechnol.* **2004**, *2*, 89.
- (26) Shinohara, H.; Inakuma, M.; Kishida, M.; Yamazaki, S.; Hashizume, T.; Sakurai, T. *J. Phys. Chem.* **1995**, *99*, 13769.
- (27) Feynman, R.; Leighton, R. B.; Sands, M. L. *The Feynman Lectures on Physics*; Addison-Wesley: Reading, MA, 1964; Commemorative Issue, Vols. 2–11.
- (28) Grabert, H.; Devoret, M. H. *Single Charge Tunneling*; NATO ASI Series; Plenum Press: New York, 1992.
- (29) Laasonen, K.; Andreoni, W.; Parrinello, M. *Science* **1992**, *258*, 1916.

NL050490Z